J Surfact Deterg (2018) **21:** 209–220
DOI 10.1002/jsde.12006

ORIGINAL ARTICLE

Hydrolytic Dephosphorylation of *p*-Nitrophenyl Diphenyl Phosphate by Alkyl Hydroxamate Ions

Neha Kandpal[1] · Hitesh K. Dewangan[1] · Rekha Nagwanshi[2] · Kallol K. Ghosh[1] · Manmohan L. Satnami[1]

Received: 16 February 2017 / Revised: 21 August 2017 / Accepted: 15 September 2017

Abstract The kinetics of the hydrolysis of *p*-nitrophenyl diphenyl phosphate (PNPDPP) by hydroxamate ions (R'(C═O)N(RO$^-$) such as octanohydroxamate (OHA$^-$) and decanohydroxamate (DHA$^-$) was investigated in dioctadecyldimethylammonium chloride (DODAC) and didodecyldimethylammonium bromide (DDAB) vesicles. The physicochemical properties of these surfactants were studied by conductivity and fluorescence measurements at 300 K. The hydrolysis of PNPDPP was studied in a vesicular system by using hydroxamate ions (OHA$^-$ and DHA$^-$) at 300 K. The different catalytic effects of hydroxamate ions for the hydrolysis of PNPDPP in the vesicles were determined. All reactions followed pseudofirst-order kinetics. The reactivity of DHA$^-$ was found to be higher than that of OHA$^-$ in the vesicular system toward the cleavage of phosphate ester. Further, the binding constants (K) and free energy change (ΔG) for the associations of PNPDPP with DODAC and DDAB vesicles were determined spectrophotometrically as well as from the Benesi–Hildebrand (B–H) plots. The pseudophase model was applied for the quantitative treatment of the kinetic data in the vesicle systems.

Keywords Vesicular surfactant · octanohydroxamate (OHA$^-$) · decanohydroxamate (DHA$^-$) · PPM

Electronic supplementary material The online version of this article (doi:10.1002/jsde.12006) contains supplementary material, which is available to authorized users.

✉ Manmohan L. Satnami
manmohanchem@gmail.com

[1] School of Studies in Chemistry, Pt. Ravishankar Shukla University, Raipur 492010, India

[2] Department of Chemistry, Government Madhav Science P. G. College, Ujjain 456010, India

J Surfact Deterg (2018) **21:** 209–220.

Introduction

Vesicles, or liposomes, first studied by Bangham in 1960, are important parts of the biological cell and control the flux of tiny molecules into and out of the cell and compartmentalize the cell contents. Vesicle self-assembly structures developed outside cells are key structures in developing biosensors and drug delivery vehicles (Alessandrini & Facci, 2014; Gunnarsson et al., 2015; Hardy, Nayak, & Zauscher, 2013; Kandpal et al., 2017; Mashaghi et al., 2014; Pross, 2004). Because of their arrangement, fluctuation, and basic properties, vesicles are also important in cosmetics and food and chemical industries (Keller, 2001; Laouini et al., 2012; Laouini, Jaafar-Maalej, Sfar, Charcosset, & Fessi1, 2011; Lian & Ho, 2001; Maurer, Fenske, & Cullis, 2001; Samad, Sultana, & Aqil, 2007). Vesicles have striking biological properties (anti-bacterial activity) as well as biocompatibility and biodegradability. They show promise in delivering encapsulated drugs to specific target sites and are especially applied in cancer treatment for sustained drug release (Uhumwangho & Okor, 2005). Vesicular properties can also be applied in the delivery of ingredients in the cosmetics industry (Betz, Aeppli, Menshutina, & Leuenberger, 2005). They offer great advantage because they are well hydrated and reduce the dryness of skin, which is a primary cause of aging. They are also being used in the treatment of hair loss; minoxidil, a vasodilator, is the active ingredient in products like Rogaine, which prevent or slow hair loss (Goymann, 2004; Lautenschläger, 2006). Vesicles or liposomes are also of importance in food products like dairy products preparation, in the stabilization of food components against degradation, and in enhancing the efficiency of

antimicrobial peptides. A typical example is the preservation of cheese, where vesicles or lipids can make the cheese ripening times shorter by 30–50% (Mozafari, Johnson, Hatziantoniou, & Demetzos, 2008; Taylor, Davidson, Bruce, & Weiss, 2005). A variety of organic reactions in micelles are considered as a consequence of their catalytic properties (Klijn & Engberts, 2003; Rispens & Engberts, 2001). Accordingly, bilayer aggregation provides distinct microenvironments for reactions. Vesicle bilayers are not as versatile as monolayers. They provide significantly more rigid interiors than micelles. Vesicle-entrapped water pools provide further distinctive environments. Some of the most investigated cationic vesicles such as didodecyldimethylammonium bromide (DDAB) and dioctadecyldimethylammonium chloride (DODAC) homologue double-chain vesicle-forming cationic lipids are extensively reported (Proverbio, Schulz, & Puig, 2002). Feitosa et al. (2006) reported interesting characteristics and behavior for the difference in chain length of these lipids (C_{18} and C_{12}). It has also been reported that cationic surfactants tend to increase the phase transition temperature (T_m) of these lipids as compared to micelle-forming nonionic surfactants (Barreleiro, Olofsson, Bonassi, & Feitosa, 2002).

Hydroxamate ions are effective deacylating and dephosphorylating agents, and their properties can be improved by comicellization with a surfactant in water. In recent studies of the reactions of nucleophilic reagents with carboxylate and phosphate esters, a significant catalytic activity has been observed. Over the pH range 6.7–11.4, bifunctional nucleophilicity of the hydroxamate ion has been documented (Satnami et al., 2010; Satnami, Karbhal, & Dewangan, 2014). Octanohydroxamic acid (OHA) and decanohydroxamic acid (DHA) are derivatives of hydroxylamine hydrochloride. They play a relevant role in biological activities as collagen inhibitors, antibiotics, and anti-inflammatory, and anticancer agents (Clare, Scozzafava, & Supuran, 2001; Kikuchi et al., 2002; Komatsu et al., 2001; Munoz, Graciani, Rodriguez, & Moya, 2003). To our knowledge, no catalytic studies have been reported with vesicles employing the kinetic properties of cationic vesicular surfactants (DODAC and DDAB) with OHA and DHA. Therefore, in this article we describe the comparative analysis of the nucleophilicity of hydroxamate ions (OHA^- and DHA^-) toward the reaction of *p*-nitrophenyl diphenyl phosphate (PNPDPP) in the presence of. DODAC and DDAB as the vesicle-forming surfactants (Chart 1).

Experimental

Materials

All the reagents, procured from Sigma-Aldrich Chemicals Pvt. Ltd. (Bangalore, India), were of the highest available grade, and used without further purification. Ultrapure (MilliQ-plus) water was used to prepare all stock solutions. OHA and DHA were synthesized by the reaction of ethyl octanoate and ethyl decanoate, respectively, with hydroxylamine hydrochloride (Roe & Swern, 1950). DODAC and DDAB were supplied by Sigma-Aldrich (Sigma-Aldrich Chemicals Pvt. Ltd., Bangalore, India) and were prepared by Fendler's procedure (Feitosa & Brown, 1997; Kano, Romero, Djermouni, Ache, & Fendler, 1979).

Vesicle Preparation

The typical procedure of vesicle preparation consists of sonic dispersions of the vesicles (DODAC and DDAB) above their gel-to-liquid crystalline phase transition temperature T_m (48 and 15 °C, for DODAC and DDAB, respectively; Soltero et al., 2000). DODAC and DDAB vesicles were spontaneously prepared by simple dilution of the surfactant (5.0 mM) in water. The DODAC/water mixture was then warmed to 60 °C (safely above the DODAC T_m = 48 °C) for complete DODAC solubilization under sonic dispersion in water using a PCI Analytics bath sonicator for 25 min (Scheme 1). Since the T_m of DDAB is lower (15 °C) (Barreleiro et al., 2002) than room temperature, it was mixed with an aqueous solvent at room temperature and kept standing for at least 24 h. After that, the samples were equilibrated to room temperature and filtered through a 0.45 μm pore size filter. To prepare the samples for kinetic measurements, stock solutions were diluted to the desired concentration. All measurements were done at the desired concentration of 1.0 mM.

Conductance Measurement

Conductivity data were collected at 300 K with a Systronics direct reading conductivity meter (Type 306). The accuracy on the measured specific conductivity (κ) is believed to be better than ±0.5%. The pure surfactant solutions were prepared by diluting the concentrated stock solution. Conductivity measurements were made at different molar ratios by subsequent addition of pure water to the concentrated solution of the surfactant mixture. Throughout the course of experiments, the temperature setting remained undisturbed.

Fluorescence Measurements

Fluorescence spectra were recorded on a Cary Eclipse fluorescence spectrophotometer. Pyrene-1-carboxaldehyde (PyCHO) was used as the fluorescence probe. During the experiments, the excitation and emission slits were fixed at 3.0 and 1.5 nm, respectively. The concentration of the probes used was 1.0 μM. Fluorescence spectra of the PyCHO solution samples were recorded in the wavelength

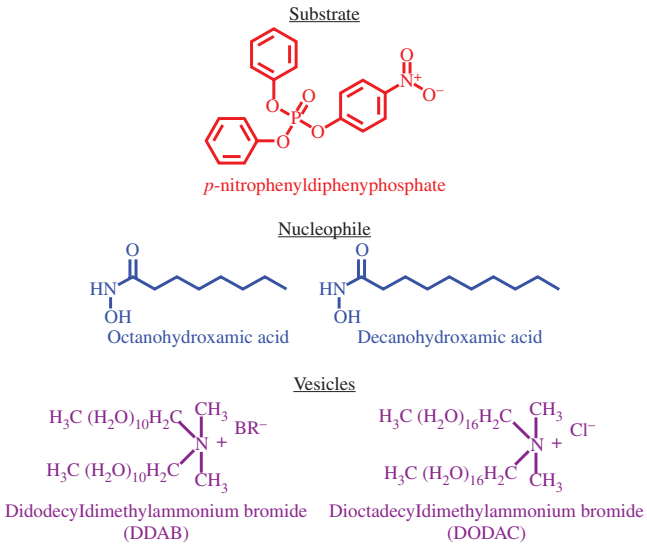

Chart 1 Compounds used in present investigation

range 375–600 nm. The excitation wavelength for PyCHO was 365 nm. To each sample solution, 10 μL of PyCHO stock solution was added. To avoid any dilution effect, the same concentration of the PyCHO probe was taken in each surfactant solution.

Kinetic Measurements

All reactions were performed at 300 K with an Evolution 300 Thermo Scientific UV–visible spectrophotometer equipped with a Peltier thermal controller. All the kinetic runs were followed under pseudofirst-order conditions in which the concentration of the nucleophiles was at least 10 times higher than the initial concentration of the substrates. The rates of nucleophilic reaction with the esters were determined by following the increase in absorption of the *p*-nitrophenoxide anion at 400 nm. All kinetic experiments were performed at an ionic strength of 0.1 M (with KCl). Phosphate and borate buffers were employed. For all of the kinetic runs, the absorbance/time results fitted very well with the first-order rate equation.

$$\ln(A_\infty - A_t) = \ln(A_\infty - A_0) - k \quad (1)$$

The pseudofirst-order rate constants (k_{obs}) were obtained from linear plots of log (A_∞ – A_t) versus time. The spectrum shows (Fig. 1) an increase in absorbance at 400 nm with the formation of the *p*-nitrophenoxide ion during the course of the reaction.

Results and Discussion

Conductance Measurements

The aggregation behaviors of DODAC and DDAB vesicles were studied using conductance measurements. The conductance of aqueous DODAC and DDAB vesicles at temperature (300 K) is presented in Fig. 2a, b. The critical vesicle concentrations (CVCs) of DODAC and DDAB have been reported as 1.0 and 2–2.5 mM (Farquhar et al., 1996; Fontana, Maria, Siani, & Robinson, 2003) respectively. The determination of the CVC of the vesicular surfactant at various concentrations of hydroxamate ions has been well documented by Satnami and coworkers (2017), who found that for all the studied systems, electrical conductivity decreased with increasing concentration of hydroxamate ions.

According to the Onsager theory of electrolyte conductivity, two linear regimes are expected in the conductivity graph, one corresponding to the prevesicular region and the other corresponding to the postvesicular region (Bhattacharya & Kumar, 2005). Usually, the degree of ionization (α), taken as the ratio of the slopes of prevesicular and postvesicular by conductivity, is linearly correlated to the surfactant concentrations. In our previous work (Kandpal et al. 2017), we also found that the CVC and degree of counterion dissociation (α) of a vesicular surfactant could be easily obtained by conductance

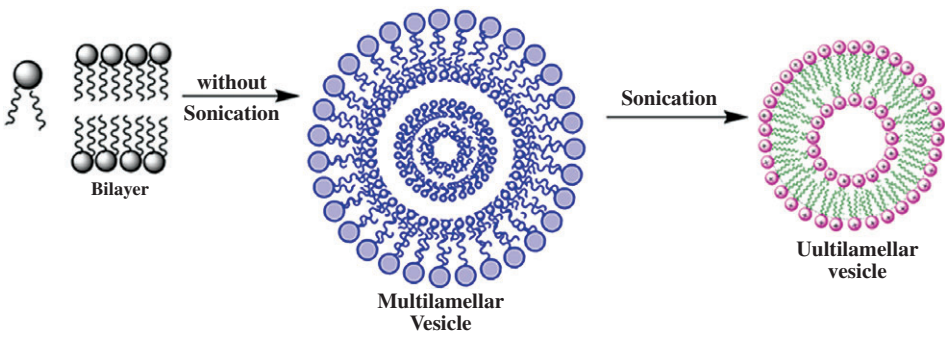

Scheme 1 Formation of vesicles

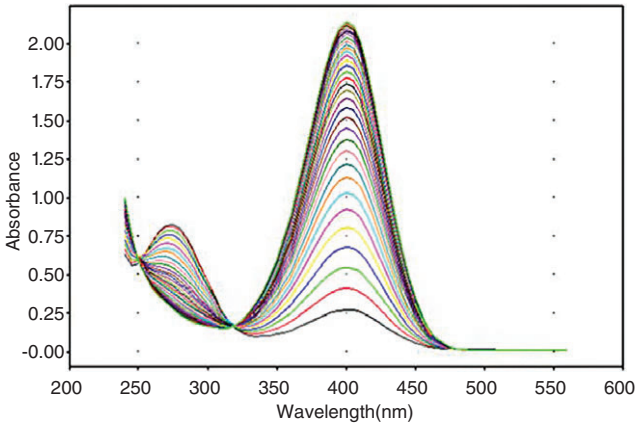

Fig. 1 UV spectra collected at different reaction times for the production of *p*-nitrophenoxide ion. Reaction condition: Temp. 27 °C; [HA^-] = 1.0 × 10^{-3} M; [PNPDPP] = 1.0 × 10^{-4} M; [DODAC and DDAB] = 0.1 × 10^{-3} M; [KCl] = 0.1 M; pH = 9.2 (borate buffer)

measurements. Table 1 shows the measured CVC of DODAC and DDAB obtained conductometrically, which shows good agreement with the reported values.

Fluorescence Measurements

In order to support the conductance results, fluorescence measurements were also made.

For determining the CVC, the probe PyCHO was used (Behera & Pandey, 2007; Fletcher, Storey, Hendrick, & Pandey, 2001). PyCHO has two types of excited singlet states (n–n* and Π–Π*), both of which show emission in solution. Figure 3 presents the PyCHO fluorescence intensity as a function of the surfactant concentration. The CVC

Table 1 Critical vesicle concentration of aqueous DODAC and DDAB vesicles obtained from conductivity and fluorescence intensity

Vesicle	CVC (mM)	
	From conductivity	From PyCHO fluorescence intensity
DODAC	1.23	1.12
DDAB	2.83	2.32

values of DODAC and DDAB are found to be in accordance with those of the conductance measurements (Table 1).

pH-Dependent Reaction

The pseudofirst-order rate constants for the reaction of PNPDPP with OHA^- and DHA^- were determined spectrophotometrically at 300 K in vesicular media. Figure 4 shows the pH-dependent pseudo-first-order rate constants on the cleavage of PNPDPP at 300 K determined at different pH values between 7.0 and11.0. The effects of positively charged vesicles on the hydrolysis of PNPDPP by hydroxamate ions were also examined. The mechanism of the above kinetics is shown in Scheme 2.

It was observed that the rate of reaction increased with the pH in the pH range 7.0–11.0 (Table S1 in Supporting Information summarizes the kinetic data obtained). The rate of reaction shows drastic changes at pH >> pK_a (Quina & Chaimovich, 1979) in the hydrolysis of PNPDPP. It is the anion of hydroxamic acid ($N–O^-$) that acts as a reactive species in the hydrolysis of esters. At higher pH, the rate constants could not be measured because the reaction was very fast.

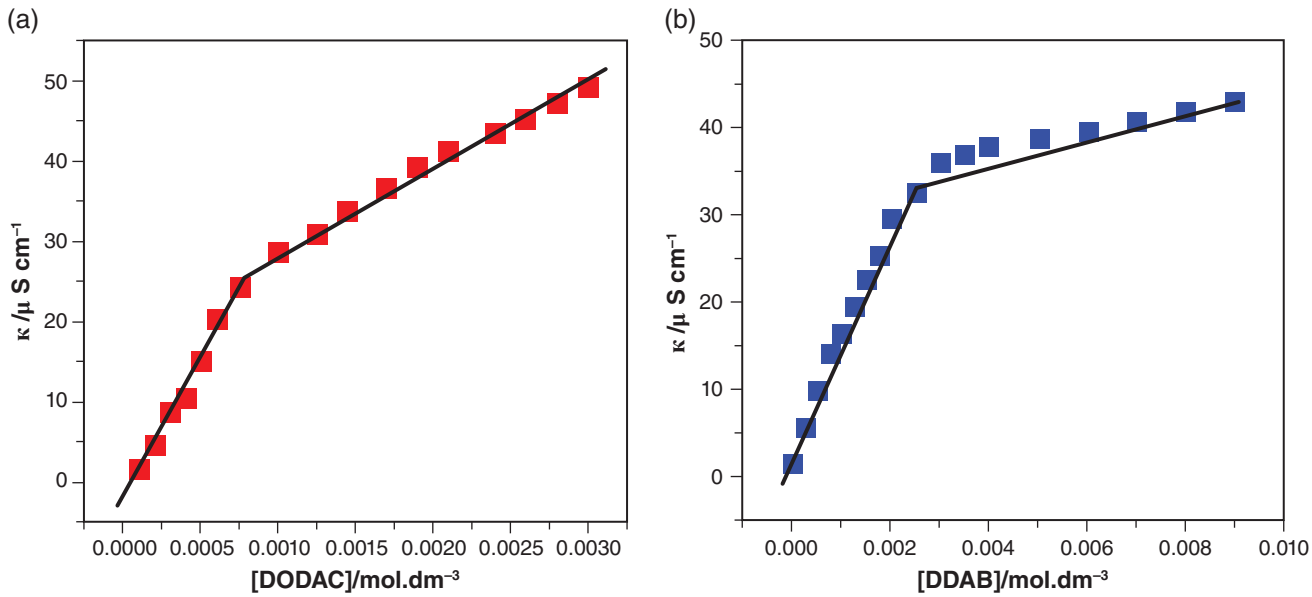

Fig. 2 Conductometric determination of CVC of (**a**) DODAC and (**b**) DDAB vesicles in the absence of hydroxamic acid

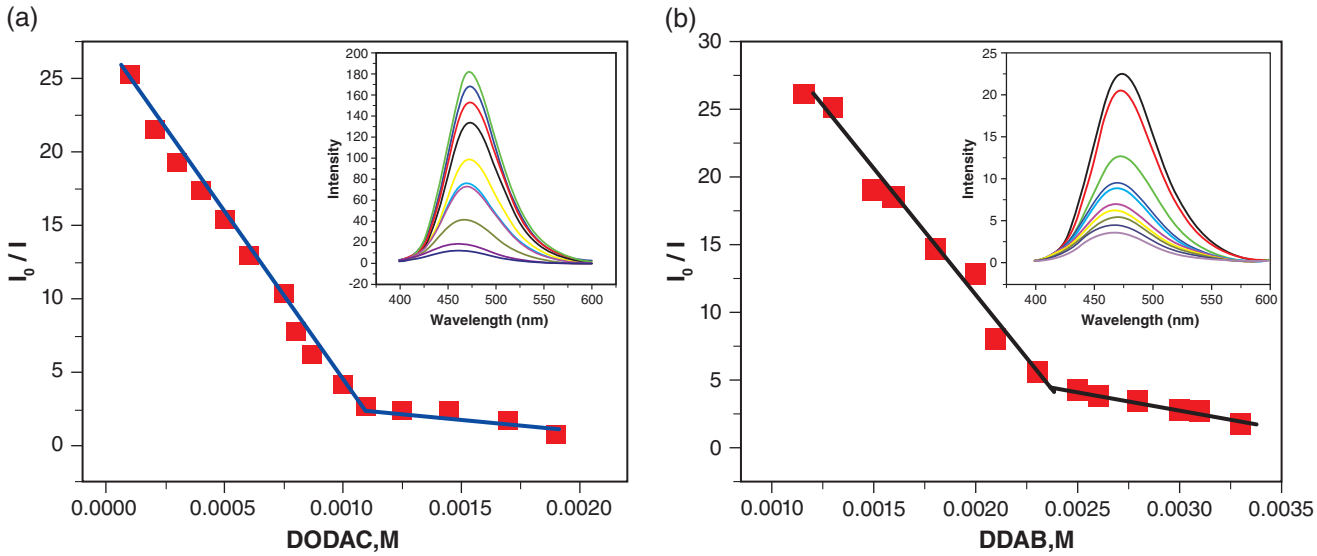

Fig. 3 Plot of fluorescence intensity (I_0/I) *versus* concentrations of (**a**) DODAC and (**b**) DDAB at 300 K. (Inset: Fluorescence emission behavior of DODAC at different concentrations in aqueous solution of pyrene1-carboxyaldehyde; excitation = 365 nm and slit widths 3.0 and 1.5 nm at 300 K)

Nucleophile-Dependent Reaction

The nucleophile concentration *versus* the first-order rate constant was determined for the reaction of PNPDPP by varying the concentration of hydroxamic acid at pH 9.2 (borate buffer). The kinetic data for the reaction of PNPDPP at different concentrations of OHA^- and DHA^- at pH 9.2 is summarized in Table S2.

Equation 2 describes the reaction of PNPDPP with nucleophiles, with k_o as defined in Eq. 3, which corresponds to the intercept in the k_{obs} *versus* $[Nu^-]$ plot. In this reaction, we used an excess of nucleophile for the reaction of the phosphate ester at 300 K and 9.2 pH.

$$k_{obs} = k_{o+} k_{Nu^-} [Nu^-] \quad (2)$$

$$k_o = k_{H2O} + k_{OH^-} [OH^-] \quad (3)$$

At high pH, the intercept is dominated by the k_{OH^-} term. The hydrolysis of PNPDPP in water is first order in the presence of the hydroxamate ion. Plotting k_{obs} *versus*

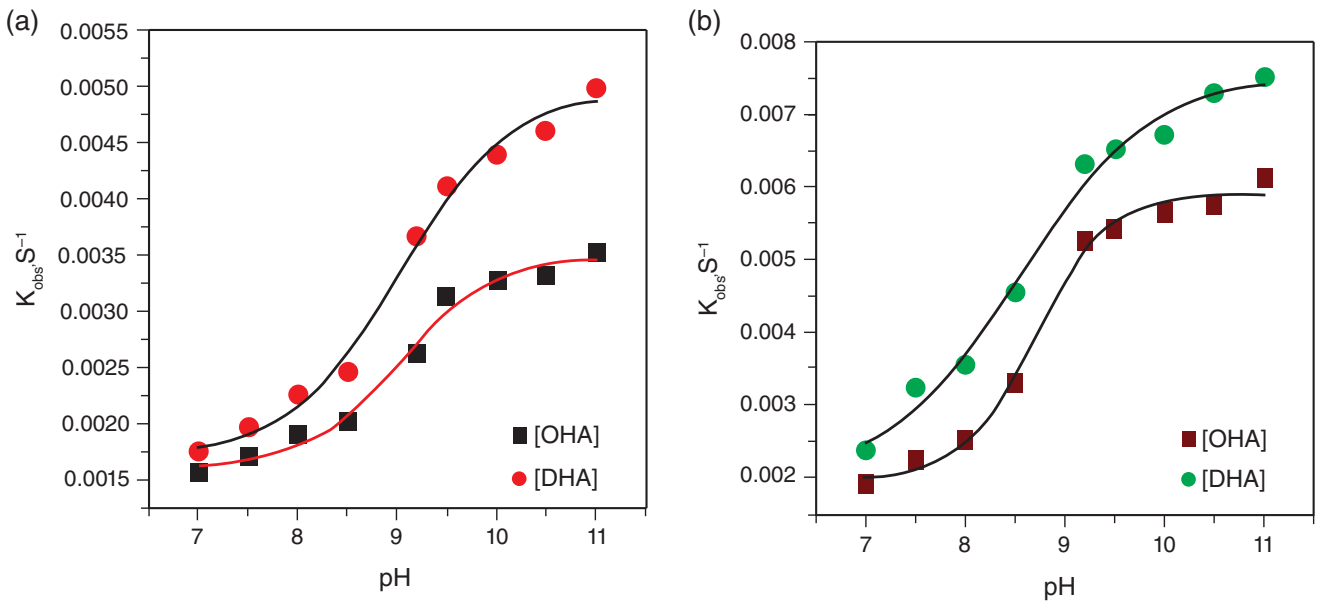

Fig. 4 Plots of k_{obs} *versus* [pH] for the reaction of hydroxamate ions with PNPDPP in (**a**) DODAC and (**b**) DDAB vesicular media. Reaction condition: [PNPDPP] = 1.0×10^{-4} M; [OHA^- and DHA^-] = 1.0×10^{-3} M; [DODAC and DDAB] = 1.0×10^{-3} M; temp. 27 °C

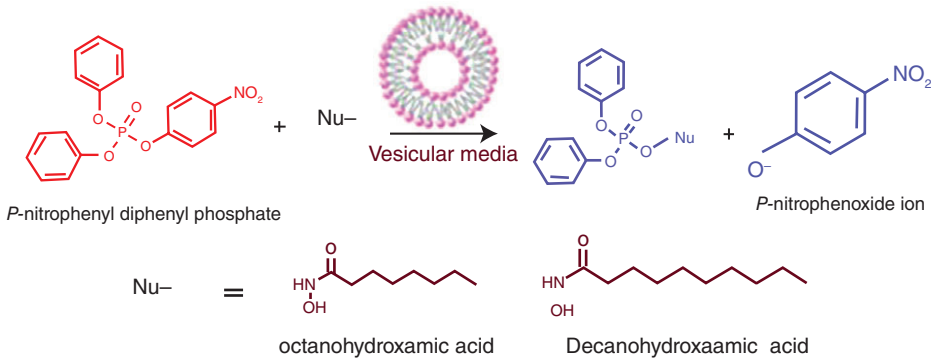

Scheme 2 Nucleophilic attack of hydroxamate ions at P═O center in the presence of vesicular media

[Nu^-] gave a straight line, as shown in Fig. 5c, with intercept k_0. A series of kinetic experiments were also performed where the nucleophile concentration was varied from 5×10^{-4} to 5×10^{-3} M at a constant vesicular concentration of 1.0×10^{-3} M. As can be seen from Fig. 5a, b, k_{obs} varied in a slightly nonlinear fashion with

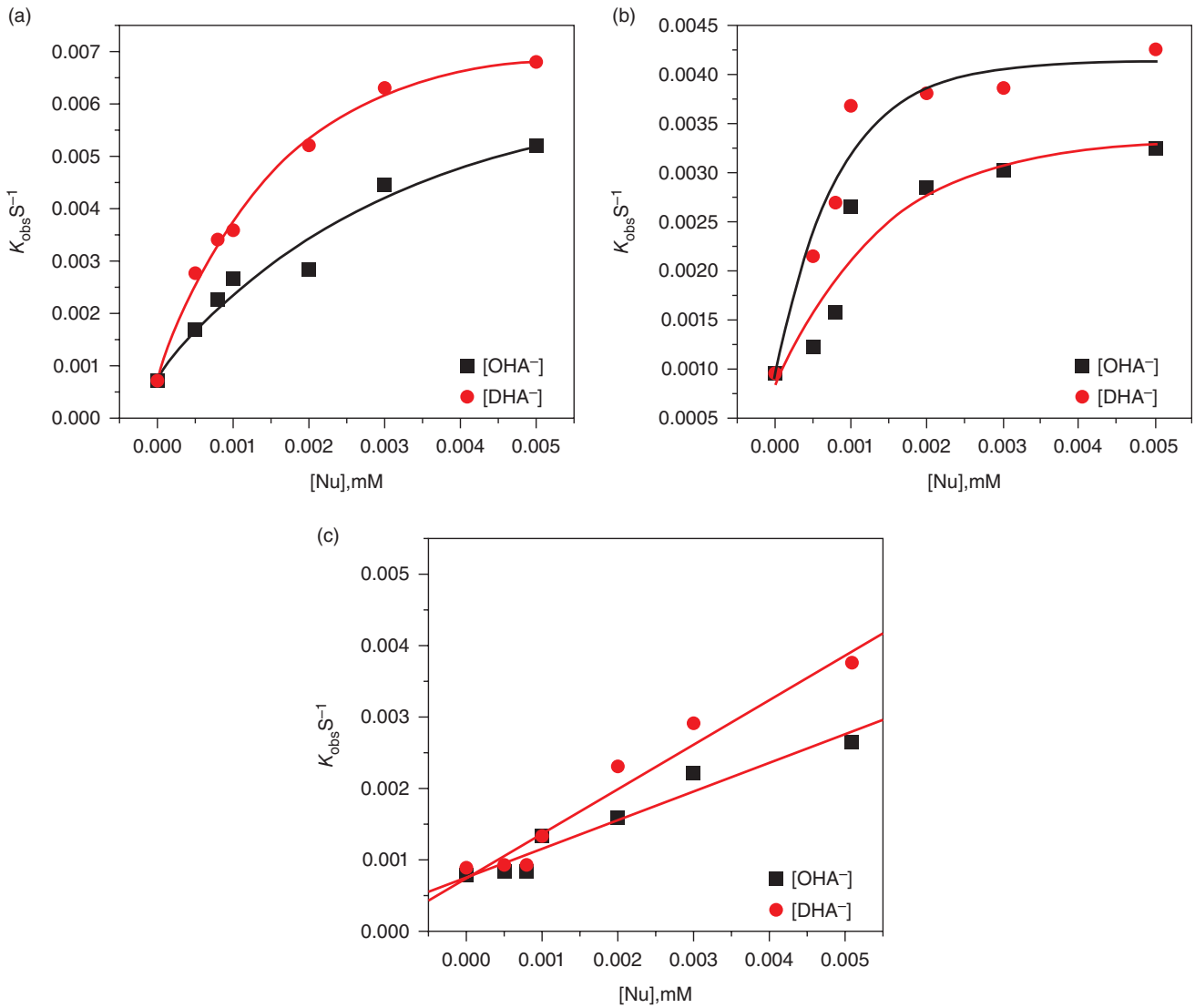

Fig. 5 Plots of k_{obs} *versus* [Nu^-] for the reaction of hydroxamate ions with PNPDPP in (**a**) DODAC, (**b**) DDAB vesicular media, and (**c**) in aqueous media. Reaction conditions: [PNPDPP] = 1.0×10^{-4} M; [DODAC and DDAB] = 1.0×10^{-3}; temp. 27 °C

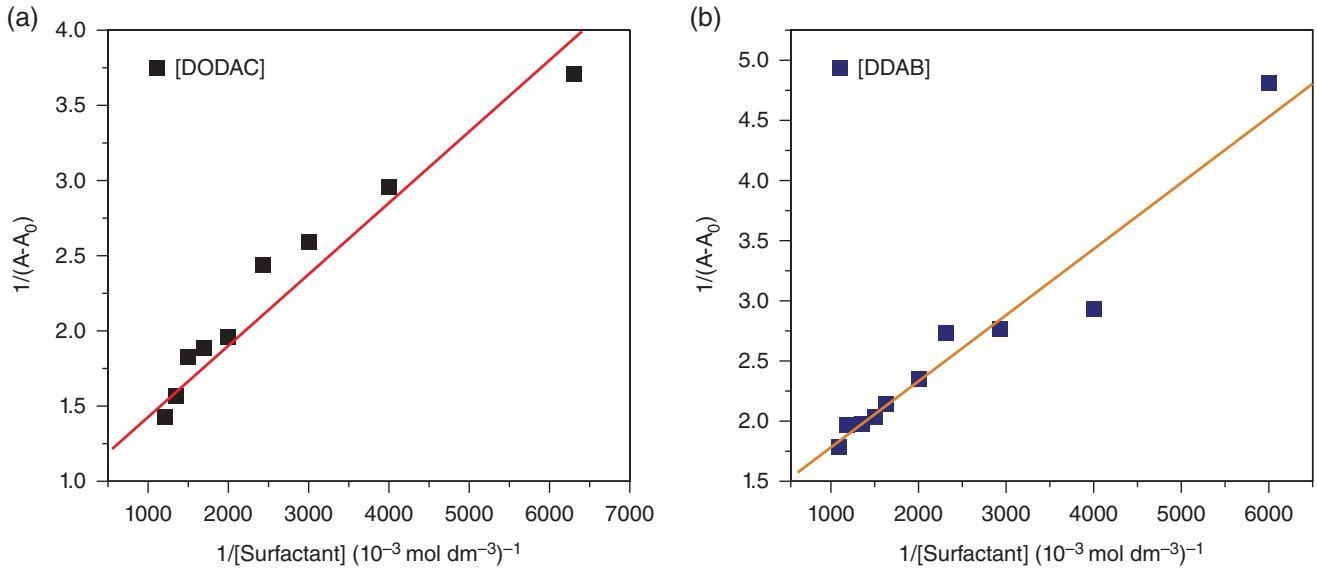

Fig. 6 Benesi–Hildebrand plot of PNPDPP using Eq. 4 for association between PNPDPP and vesicular surfactants (**a**) DODAC and (**b**) DDAB

[OH^-] (Gracia-Rio, Leis, Mejuto, & Pena, 1994; Tanuli & Fendler, 1981).

The vesicles start aggregating as a result of saturation with OH^- ions. OH^- ions have high charge density and they neutralize the charge of the polar heads of ions, resulting in the structural change of the system significantly compared to other microheterogeneous media, thereby inducing the vesicles to aggregate (Kunitake, Hirotaka, & Okahata, 1983; Kunitake, Okahata, Ando, Shinkai, & Hirakawa, 1980; Patel, Bijma, & Engberts, 1994). The membrane rigidity is due to the relative inefficiency of the bilayers with two C_{18}. This anomalous catalytic effect has been reported in the literature and varies with the ammonium bilayer membrane rigidity (Chaimovich, Bonilha, Zanette, & Cuccovia, 1984). It can be seen that DHA^- is more reactive than OHA^- at pH 9.2 for attacking the phosphate center of PNPDPP. Finally, DODAC is found to be less reactive than DDAB because of its membrane rigidity.

Determination of Binding Constant

The distribution or "binding" constants of PNPDPP to the cationic vesicular systems were estimated from the Benesi–Hildebrand (B–H) equation 4 (Benesi & Hildebrand, 1949) as follows:

$$1/A - A_0 = 1/K\,(A_{max} - A_0)\,[\text{surfactant}] + 1/A_{max} - A_0. \quad (4)$$

where A_0, A, and A_{max} are the absorbance in the absence, at intermediate concentration, and at infinite concentration of the surfactant, respectively, and K is the binding constant. A series of solutions (3 mL each total volume) were prepared of varying the cationic surfactant concentration (0–0.8 mM) without the added buffer. Next, small amounts of substrate (PNPDPP) stock solution (20 µL of 0.0015 mM) were successively added to each of the surfactant-containing solutions. After mixing, an aliquot (3 mL) was transferred to a quartz cuvette and the absorbance recorded in the 250–300 nm wavelength region. The plot of $1/(A - A_0)$ *versus* 1/[surfactant] gives straight lines (Fig. 6), which indicates the formation of the complex between the substrate and vesicles (DODAC and DDAB). The values of the binding constants of PNPDPP obtained from the slope of the B–H plot (Fig. 6) are 4.790×10^4 and 5.492×10^4 mol dm^{-3} for DODAC and DDAB vesicles, respectively.

Table 2 Estimated binding constant (K), free energy changes for the substrate–vesicle complexation (ΔG), and the correlation coefficients (R) for DODAC and DDAB vesicles

Substrate–vesicle complex	$(K)\ 10^4$ (mol dm^{-3})	ΔG (kJ mol^{-1})	R
PNPDPP + DODAC	4.790	−30.07	0.9601
PNPDPP + DDAB	5.492	−42.48	0.9727

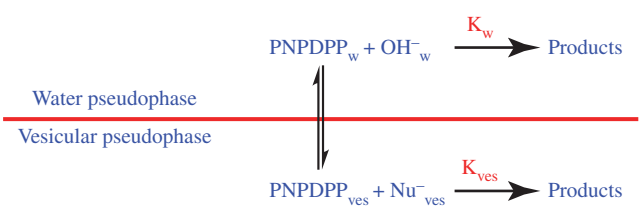

Scheme 3 Quantitative treatment of vesicles: the pseudophase model

Table 3 Kinetic parameters obtained by applying the pseudophase model for the nucleophilic reaction of PNPDPP in the presence of cationic vesicle DODAC

Nu^-	k_2^w (M^{-1} s^{-1})	K_m^{Nu} (M^{-1})	$k_2^m/\overline{V}$ (M^{-1} s^{-1})
		DODAC	DODAC
OHA^-	0.396	58.47 ± 12.56	(0.0735 ± 0.016)
DHA^-	0.828	94.94 ± 13.48	(0.0898 ± 0.4)

Table 4 Kinetic parameters obtained by applying pseudophase model for the nucleophilic reaction of PNPDPP in the presence of cationic vesicle DDAB

Nu^-	k_2^w (M^{-1} s^{-1})	K_m^{Nu} (M^{-1})	$k_2^m/\overline{V}$ (M^{-1} s^{-1})
		DDAB	DDAB
OHA^-	0.396	220 ± 24.37	0.0255
DHA^-	0.828	57.71 ± 9.95	0.0787

From the values of K, the free energy change (ΔG) for this process of complexation can be obtained by employing the relation $\Delta G = -RT \ln K$. Table 2 shows the values of K and ΔG obtained from spectroscopic measurements. The negative value of ΔG shows that the substrate–vesicle complexation is energetically favorable. As can be observed from the values of K, the binding of PNPDPP is stronger for DODAC than DDAB because of the slight difference in their hydrophobicity, leading to their different binding abilities.

Quantitative Treatment of PNPDPP by Vesicular Surfactant: Pseudophase Model

The kinetic rate data can be quantitatively analyzed using the pseudophase model (PPM) (Bunton, 1997), assuming two pseudophases in which the reaction is treated as occurring in a vesicular pseudophase (representing the DODAC/DDAB bilayer) and an aqueous pseudophase and assuming an equilibrium distribution of the substrate between both pseudophases. The overall reaction rate is the sum of the rate in each pseudophase and depends on the rate constants and reactant concentrations in each pseudophase, as shown in Scheme 3, where subscripts w and ves denote the aqueous and vesicular pseudophases, and k_w and k_{ves} are the bimolecular rate constants in the respective pseudophases. This model leads to the following equation:

$$K_{obs} = \frac{k_2^w + \left(k_2^{ves}/V\right)K_{ves}^{substrate}K_{ves}^{Nu^-}|D_n|}{\left(1 + K_{ves}^{Substrate}|D_n|\right)\left(1 + K_{ves}^{Nu^-}|D_n|\right)}[Nu^-]_T \quad (5)$$

Scheme 2 can be used for applying the PPM. In this model, subscripts w and m signify aqueous and vesicular pseudophases, respectively, and D_n represents the vesicularized surfactant, which, as shown in Scheme 2, considers the distribution of substrate between the aqueous and vesicular pseudophases. The different reactivities in the aqueous and vesicular pseudophases have been taken into account through the corresponding second-order rate constants k_2^w and k_2^{ves}. We assume V to be equal to the partial molar volume of the interfacial region in the vesicular pseudophase, taken as 0.56 M^{-1} (Kawamuro, Chaimovich, Abuin, Lissi, & Cuccovia, 1991). By applying the PPM (Tables 3 and 4 summarize the kinetic data), we have calculated the bimolecular rate constant within the bilayer, k_2^{ves}. In both the vesicles, k_2^{ves} is higher than the rate constant in water, possibly because of the reduced micropolarity at the vesicular pseudophase.

The effects of different vesicle-forming surfactants (DDAB and DODAC) at a constant pH 9.2 were studied at

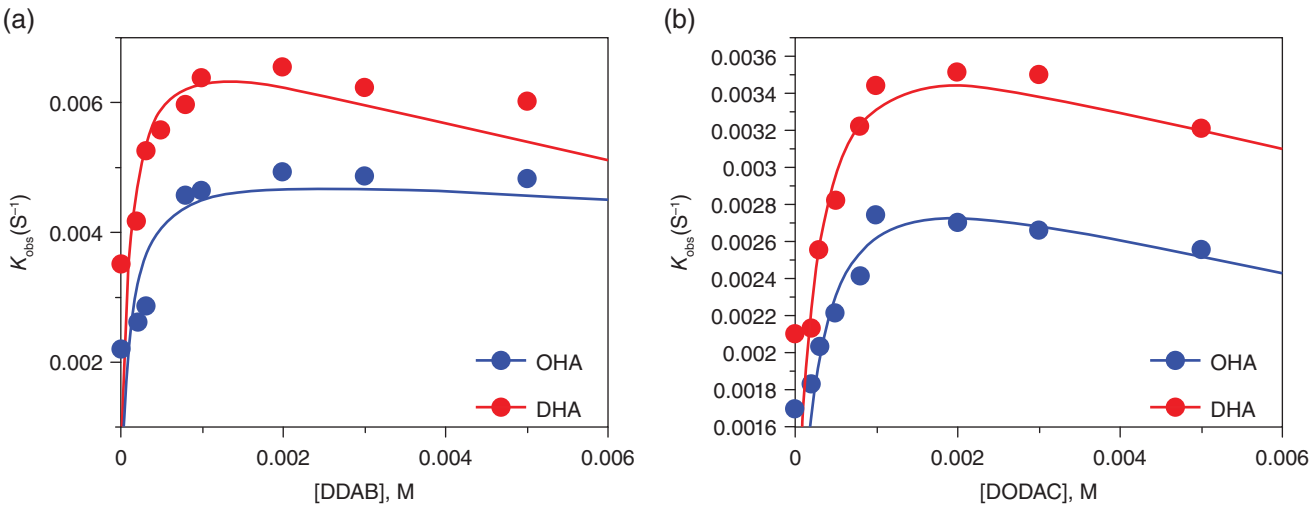

Fig. 7 Simulated rate-surfactant profile for the reaction of PNPDPP with OHA^- and DHA^- in (**a**) DDAB and (**b**) DODAC vesicular media. (The lines represent the best fit to the pseudophase model.) Reaction condition: [PNPDPP] = 1.0×10^{-4} M; [nu^-] = 1.0×10^{-3} M; [KCl] = 0.1 M; pH = 9.2 (borate buffer); temp. 27 °C

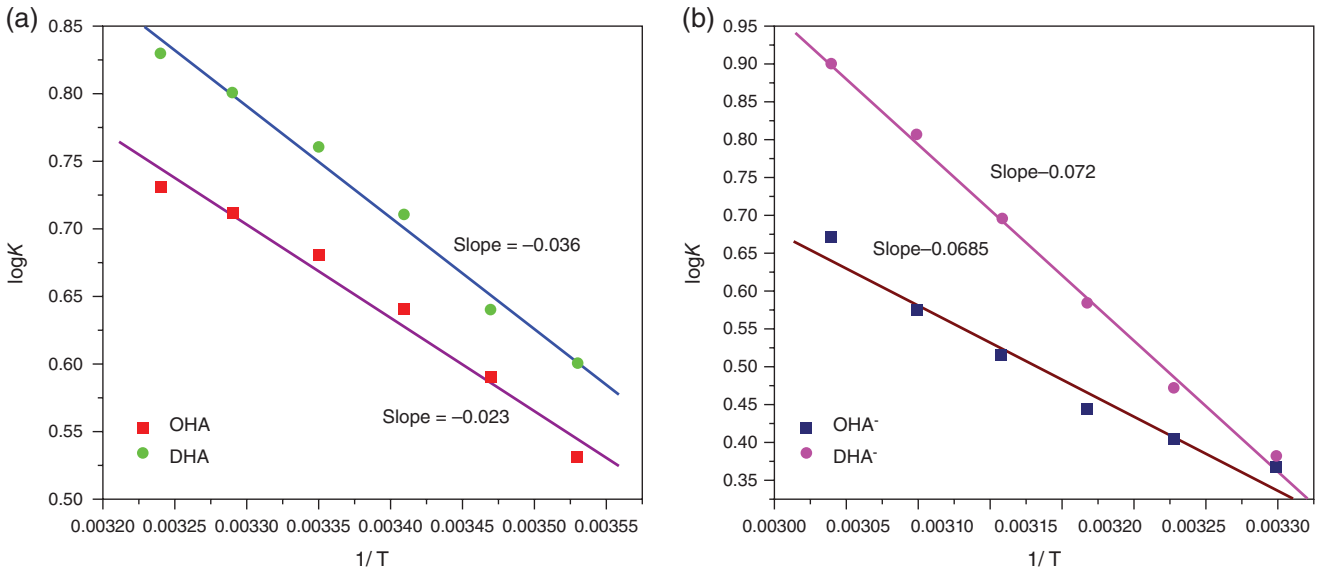

Fig. 8 Arrhenius plot for the hydrolysis of PNPDPP in the presence of (**a**) DODAC and (**b**) DDAB vesicles

different vesicular concentrations ranging from 0.2 to 5 mM. Table S3 summarizes the data obtained. As can be seen from Fig. 7**,** on increasing the amount of vesicles in the medium, the catalytic effect also increases up to a maximum value when all PNPDPP was coupled to the vesicles. A further increase in the DODAC concentration decreased the reaction rate through the displacement of reactive ions (OH^-) from the bilayer surface by the effect of the increased concentration of nonreactive ions (Cl^-). The partial dehydration of OH^- and the lower local polarity are considered to contribute significantly to the catalysis of the DODAC vesicles. The catalytic efficiency of the vesicles at 300 K confirms that DDAB vesicles are more reactive than DODAC vesicles.

Activation Parameters

The activation parameters, i.e., the enthalpy of activation (ΔH°), Gibbs energy of activation (ΔG°), and entropy of activation (ΔS°), were determined for the hydrolysis of PNPDPP by hydroxamate ions (OHA^- and DHA^-) in the presence of DODAC and DDAB vesicles. The enthalpies and entropies of activation were calculated using Eq. 6 (Laidler & Meiser, 1999):

$$\ln(k_{ves}h/k_BT) = \Delta S^\circ/R - \Delta H^\circ/\mathrm{RT}. \quad (6)$$

in which k_B is the Boltzmann constant (1.3807×10^{-23} J K^{-1}), h is the Planck constant (6.626×10^{-34} Js), T is the absolute temperature, R is the gas constant, ΔS° is the entropy of activation, and ΔH° is the enthalpy of activation. The activation energy can be calculated by the Arrhenius equation (Al-Ghouti, Khrailsheh, Ahmad, & Allen, 2005).

$$\ln k_2 = \ln k_0 - E_a/RT. \quad (7)$$

where k_2 is the pseudosecond-order constant (mol^{-1} min^{-1}), k_0 is the rate constant (g mol^{-1} min^{-1}), E_a is activation energy (J mol^{-1}), R is the gas constant (8.314 J mol^{-1} K^{-1}), and T is the solution temperature (K). Plotting $\ln k_2$ against the reciprocal of temperature gives a straight line, as shown in Fig. 8, the slope of which is $-E_a/R$.

The data were recorded below and above their main phase transition temperature. From the data, we expected a higher rate enhancement with increasing chain length and an accompanying lower micropolarity at the vesicular binding sites. We know that DODAC and DDAB self-assemble spontaneously above their gel-to-liquid crystalline phase transition temperature (T_m = 48 and 20 °C, respectively). Further, shorter alkyl chains (i.e., DDAB) result in weaker van der Waals attraction forces between them within domains of bilayers, and longer alkyl chains (i.e., DODAC) result in stronger van der Waals attraction

Table 5 Activation parameters for the hydrolysis of PNPDPP in the presence of DODAC and DDAB vesicles at 300 K

Nucleophiles	DODAC			DDAB		
	ΔH^* (kJ mol^{-1})	ΔG^* (kJ mol^{-1})	$-\Delta S^*$ (J K^{-1} mol^{-1})	ΔH^* (kJ mol^{-1})	ΔG^* (kJ mol^{-1})	$-\Delta S^*$ (J K^{-1} mol^{-1})
[OHA^-]	15.86	21.69	37.80	32.37	44.19	43.55
[DHA^-]	10.49	19.58	28.56	30.54	41.67	36.97

forces between vesicular bilayers. Here, we have calculated the activation parameters of vesicles at 300 K. As can be seen from the activation parameters data, vesicles containing DODAC have a T_m that lies above 35 °C. Gibbs energy of activation may be written in terms of entropy and enthalpy of activation as

$$\Delta G^{\circ} = \Delta H^{0} - T\Delta S. \quad (8)$$

Although the values given for ΔG° and other activation parameters were calculated at 35 °C, these data were obtained using the slope for the temperature above T_m. This is the reason why the activation parameter for DDAB is larger than that of DODAC vesicles. Further, the values of the entropy of activation (ΔS°) are negative as well, indicating that the vesicle formation process is endothermic. The enthalpy of activation (ΔH°), Gibbs energy of activation (ΔG°), and entropy of activation (ΔS°) are shown in Table 5.

Conclusions

In summary, we observed that vesicles are more effective reaction media than micelles, primarily due to the less polar microenvironment at the substrate binding sites for the deprotonation of the nucleophile. We have correlated the reactivity of different vesicles, i.e., DODAC and DDAB, with the effect of pH, nucleophile, and vesicle concentration on the rate of hydrolysis of PNPDPP. The CVC of DODAC and DDAB vesicles was found to be 1 and 2.5 mM, respectively, which was confirmed by both conductometric and fluorimetric techniques. The activation parameters for the reaction of PNPDPP in vesicles were calculated at 300 K. By comparing both the data, we found that the values of the activation parameters of DDAB are higher than those of DODAC vesicles, which is consistent with the lower micropolarity at the DODAC vesicular surface than DDAB. The results from conductivity and fluorimetry are in good agreement. On the basis of all these results, we concluded that DDAB was more reactive than DODAC, and it was clear that, with increasing chain length, the micropolarity at the vesicular binding sites became low. Also, from the higher-phase transition temperature of DODAC vesicles, the structure is in a rigid state at the reaction temperature, whereas the DDAB vesicles are in a less rigid liquid-crystalline state. In this study, we found that the nucleophilic reactivity of hydroxamate ions is higher with the cationic vesicular media toward ester cleavage than with aqueous media. It is evident from the kinetic data that DHA shows higher reactivity than OHA and that the rate of reaction increases with increasing concentration of hydroxamate ions. Thus, apart from its implication as a biomembrane model, the bilayer membrane provides reaction sites whose microenvironments can be varied over a range that is much wider than those of the conventional fluid micelle.

Acknowledgements This work was supported by the Chhattisgarh Council of Science and Technology (CCOST, grant no. 1104/CCOST/MRP/15, Raipur, 2015, dated 04.09.2015).The authors wish to thank the Head, School of Studies in Chemistry, Pt. Ravishankar Shukla University, Raipur, for providing the lab facilities.

References

Alessandrini, A., & Facci, P. (2014) Phase transitions in supported lipid bilayers studied by AFM. *Soft Matter*, **10**:7145–7164.

Al-Ghouti, M., Khrailsheh, M. A. M., Ahmad, M. N. M., & Allen, S. (2005) Thermodynamic behaviour and the effect of temperature on the removal of dyes from aqueous solution using modified diatomite: A kinetic study. *Journal of Colloid and Interface Science*, **287**:6–13.

Barreleiro, P. C. A., Olofsson, G., Bonassi, N. M., & Feitosa, E. (2002) Interaction of octaethylene glycol n-dodecylmonother with dioctadecyldimethylammonium bromide and chloride vesicles. *Langmuir*, **18**:1024–1029.

Behera, K., & Pandey, S. (2007) Concentration-dependent dual behavior of hydrophilic ionic liquid in changing properties of aqueous sodium dodecyl sulfate. *The Journal of Physical Chemistry. B*, **111**:13307–13315.

Benesi, H. A., & Hildebrand, J. H. (1949) A spectrophotometric investigation of the interaction of iodine with aromatic hydrocarbons. *Journal of the American Chemical Society*, **71**:2703–2707.

Betz, G., Aeppli, A., Menshutina, N., & Leuenberger, H. (2005) In vivo comparison of various liposome formulations for cosmetic application. *International Journal of Pharmaceutics*, **296**:44–54.

Bhattacharya, S., & Kumar, V. P. (2005) Ester cleavage properties of synthetic hydroxybenzotriazoles in cationic monovalent and gemini surfactant micelles. *Langmuir*, **21**:71–78.

Bunton, C. A. (1997) Reactivity in aqueous association colloids descriptive utility of the peudophase model. *Journal of Molecular Liquids*, **7**:231–249.

Chaimovich, H., Bonilha, J. B. S., Zanette, D., & Cuccovia, I. M. (1984) Analysis of the effect of micelles and vesicles on the reactivity of nucleophiles derived from the dissociation of weak acids. In K. L. Mittal & B. Lindman (Eds.), *Surfactants in solution* (Vol. **2**, pp. 1121–1138). New York, NY: Plenum Press.

Clare, B. W., Scozzafava, A., & Supuran, C. T. (2001) Protease inhibitors: Synthesis of a series of bacterial collagenase inhibitors of the sulfonyl amino acyl hydroxamate type. *Journal of Medicinal Chemistry*, **44**:2253–2258.

Farquhar, K. D., Misran, M., Robinson, B. H., Steytler, D. C., Morini, P., Garrett, P. R., & Holzwarth, J. F. (1996) Counterion binding and regulation of interactions between charged bilayers. *The Journal of Physical Chemistry*, **100**:16268–16274.

Feitosa, E., & Brown, W. (1997) Fragment and vesicle structures in sonicated dispersions of dioctadecyldimethylammonium bromide. *Langmuir*, **13**:4810–4816.

Feitosa, E., Fernanda, R. A., Niemiec, A., Elisabete, C. D., Elisabete, M. S., & Baptista, A. L. F. (2006) Catioic liposomes in mixed didodecyldimethylammonium bromide aqueous dispersions studied by differential scanning calorimetry, Nile red fluorescence, and turbidity. *Langmuir*, **22**:3579–3585.

Fletcher, K. A., Storey, I. A., Hendrick, A. E., & Pandey, S. (2001) Behavior of the solvatochromic probes Reichardt's dye, pyrene,

dansylamide, Nile red and 1-pyrenecarbaldehyde within the room-temperature ionic liquid bmimPF6. *Green Chemistry*, **3**: 210–215.

Fontana, A., Maria, D. P., Siani, G., & Robinson, H. B. (2003) Kinetics of breakdown of vesicles from didodecyldimethylammonium bromide induced by single chain surfactants and by osmotic stress in aqueous solution. *Colloids and Surfaces B: Biointerfaces*, **32**: 365–374.

Goymann, M. (2004) Physicochemical characterization of colloidal drug delivery systems such as reverse micelles, vesicles, liquid crystals and nanoparticles for topical administration. *European Journal of Pharmaceutics and Biopharmaceutics*, **58**:343–356.

Gracia-Rio, L., Leis, J. R., Mejuto, J. C., & Pena, M. E. (1994) Effects of additives on the internal dynamics and properties of water/AOT/isooctane microemulsions. *Langmuir*, **10**:1676–1683.

Gunnarsson, A., Snijder, A., Hicks, J., Gunnarsson, J., Hook, F., & Geschwindner, S. (2015) Drug discovery at the single molecule level: Inhibition-in-solution assay of membrane-reconstituted β-secretase using single-molecule imaging. *Analytical Chemistry*, **87**:4100–4103.

Hardy, G. J., Nayak, R., & Zauscher, S. (2013) Model cell membranes: Techniques to form complex biomimetic supported lipid bilayers via vesicle fusion. *Current Opinion in Colloid & Interface Science*, **18**:448–458.

Kandpal, N., Dewangan, H. K., Nagwanshi, R., Vaishanav, S., Ghosh, K. K., & Satnami, M. L. (2017) Reactivity of hydroxamate ions in cationic vesicular media for the cleavage of carboxylate esters. *Journal of Surfactants and Detergents*, **20**:331–340.

Kano, K., Romero, A., Djermouni, B., Ache, H., & Fendler, J. H. (1979) Characterization of surfactant vesicles as membrane mimetic agents. *Journal of the American Chemical Society*, **101**:4030–4037.

Kawamuro, M. K., Chaimovich, H., Abuin, E. B., Lissi, E. A., & Cuccovia, I. M. (1991) Evidence that the effects of synthetic amphiphile vesicles on reaction rates depend on vesicle size. *The Journal of Physical Chemistry*, **95**:1458–1463.

Keller, B. (2001) Liposomes in nutrition. *Trends in Food Science and Technology*, **12**:25–31.

Kikuchi, T., Itoh, F., Toyota, M., Suzuki, H., Yamamoto, H., Fujita, M., … Imai, K. (2002) Aberrant methylation and histone deacetylation of cyclooxygenase 2 in gastric cancer. *International Journal of Cancer*, **97**:272–277.

Klijn, J. E., & Engberts, J. B. F. N. (2003) Kemp elimination in membrane mimetic reaction media: probing catalytic properties of catanionic vesicles formed from double-tailed amphiphiles. *Journal of the American Chemical Society*, **125**:1825–1833.

Komatsu, Y., Tomizaki, K. Y., Tsukamoto, K. T., Nishino, N., Sato, S., Yamori, T., … Hayashi, H. (2001) Cyclic hydroxamic-acid-containing peptide 31, a potent synthetic histone deacetylase inhibitor with antitumor activity. *Cancer Research*, **61**: 4459–4466.

Kunitake, T., Hirotaka, I., & Okahata, Y. (1983) Phase separation and reactivity changes of phenyl ester substrate and imidazole catalyst in the dialkylammonium bilayer membrane. *Journal of the American Chemical Society*, **105**:6070–6078.

Kunitake, Y., Okahata, Y., Ando, R., Shinkai, S., & Hirakawa, S. (1980) Decarboxylation of 6-nitrobenzisoxazole-3-carboxylate catalyzed by ammonium bilayer membranes: A comparison of the catalytic behavior of micelles, bilayer membranes, and other aqueous aggregates. *Journal of the American Chemical Society*, **102**: 7877–7881.

Laidler, K. J., & Meiser, J. M. (1999) *Thermodynamic and adsorption studies of dye (rhodamine-b) onto natural diatomite-P* (Vol. **852**). New York, NY: Houghton Mifflin.

Laouini, A., Jaafar-Maalej, C., Limayem-Blouza, I., Sfar, S., Charcosset, C., & Fessi, H. (2012) Preparation, characterization and applications of liposomes: State of the art. *Journal of Colloid Science and Biotechnology*, **1**:147–168.

Laouini, A., Jaafar-Maalej, C., Sfar, S., Charcosset, C., & Fessi1, H. (2011) Liposome preparation using a hollow fibre membrane contactor-application to spironolactone encapsulation. *International Journal of Pharmaceutics*, **415**:53–61.

Lautenschläger, H. (2006) *Liposomes handbook of cosmetic science and technology* (pp. 155–163). Boca Raton, FL: Taylor and Francis Group/CRC Press.

Lian, T., & Ho, R. J. (2001) Trends and developments in liposome drug delivery systems. *Journal of Pharmaceutical Sciences*, **90**: 667–680.

Mashaghi, A., Mashaghi, S., Reviakine, I., Heeren, R. M., Sandoghdar, V., & Bonn, M. (2014) Label-free characterization of biomembranes: From structure to dynamics. *Chemical Society Reviews*, **43**:887–900.

Maurer, N., Fenske, D. B., & Cullis, P. R. (2001) Developments in liposomal drug delivery systems. *Expert Opinion on Biological Therapy*, **1**:923–947.

Mozafari, M. R., Johnson, C., Hatziantoniou, S., & Demetzos, C. (2008) Nanoliposomes and their applications in food nanotechnology. *Journal of Liposome Research*, **18**:309–327.

Munoz, M., Graciani, M. D. M., Rodriguez, A., & Moya, M. L. (2003) Influence of the addition of alcohol on the reaction methyl-4-nitrobenzenesulfonate + Br^- in tetradecyltrimethylammonium bromide aqueous micellar solutions. *Journal of Colloid and Interface Science*, **266**:208–214.

Patel, M., Bijma, K., & Engberts, J. B. F. N. (1994) Decarboxylation of 6-nitrobenzisoxazole-3-carboxylate. Enthalpy-entropy compensation in micellar and vesicular catalysis: A novel analysis of contrasting rate variations. *Langmuir*, **10**:2491–2492.

Pross, A. (2004) Casuation and the origin of life: Metabolism or replication first? *Bios*, **34**:307–321.

Proverbio, Z. E., Schulz, P. C., & Puig, J. E. (2002) Aggregation of the aqueous dodecyltrimethylammonium bromide–didodecyldimethylammonium bromide system at low concentration. *Colloid & Polymer Science*, **280**:1045–1052.

Quina, F. H., & Chaimovich, H. (1979) Ion exchange in micellar solutions: Conceptual framework for ion exchange in micellar solutions. *The Journal of Physical Chemistry*, **83**:1844–1850.

Rispens, T., & Engberts, J. B. F. N. (2001) Efficient catalysis of a Diels-Alder reaction by metallo-vesicles in aqueous solution. *Organic Letters*, **3**:941–943.

Roe, E. T., & Swern, D. (1950) Determination of long-chain hydroxamic acids. *Analytical Chemistry*, **22**:1160–1162.

Samad, A., Sultana, Y., & Aqil, M. (2007) Liposomal drug delivery systems: An update review. *Current Drug Delivery*, **4**: 297–305.

Satnami, M. L., Dhritlahre, S., Nagwanshi, R., Karbhal, I., Ghosh, K. K., & Nome, F. (2010) Nucleophilic attack of salicylhydroxamate ion at C=O and P=O centers in catioic micellar media. *The Journal of Physical Chemistry. B*, **114**: 16759–16765.

Satnami, M. L., Karbhal, I., & Dewangan, H. K. (2014) *O*-Nucleophilicity of hydroxamate ions for cleavage of carboxylate and phosphate esters in cationic micelles. *International Journal of Chemical Kinetics*, **46**:419–432.

Soltero, J. F. A., Bautista, F., Pecina, E., Puig, J. E., Manero, O., Proverbio, Z., & Schulz, P. C. (2000) Rheological behavior in the didodecyldimethylammonium bromide/water system. *Colloid & Polymer Science*, **278**:37–47.

Tanuli, M. S., & Fendler, J. H. (1981, 1994) Aspects of artificial photosynthesis. Photosensitized electron transfer across bilayers, charge separation, and hydrogen production in anionic surfactant vesicles. *Journal of the American Chemical Society*, **103**: 2507–2513.

Taylor, T. M., Davidson, P. M., Bruce, B. D., & Weiss, J. (2005) Liposomal nanocapsules in food science and agriculture. *Critical Reviews in Food Science and Nutrition*, **45**:587–605.

Uhumwangho, M., & Okor, R. (2005) Current trends in the production and biomedical applications of liposomes :A review. *Journal of Medicine and Biomedical Research*, **4**:9–21.

Biographies

Neha Kandpal has completed the M.Phil. degree and is presently working as a research scholar with the CCOST Project, under the supervision of Dr. Manmohan L. Satnami at the School of Studies in Chemistry, Pt. Ravishankar Shukla University, Raipur, India. Her research topic is "hydrolytic cleavage of organophosphorus-based pesticides in self-organized media."

Hitesh K. Dewangan has completed the M.Phil. degree and is presently working as a research scholar with the DST Fast Track Project under the supervision of Dr. Manmohan L. Satnami at the School of Studies in Chemistry, Pt. Ravishankar Shukla University, Raipur, India. His research topic is "O- nucleophilicity of hydroxamic acids and esterolytic cleavage of some simulants of chemical warfare agents and organophosphorus pesticides."

Rekha Nagwanshi is an Assistant Professor with the Department of Chemistry, Government Madhav Science P. G. College, Ujjain, India. Recently, she has been awarded a U.G.C. Research Award, New Delhi, India. Her research interests include inorganic synthesis.

Kallol K. Ghosh is an Assistant Professor with the School of Studies in Chemistry, Pt. Ravishankar Shukla University, Raipur, India. His research is focused on micellar catalysis, solubility of aromatic hydrocarbons, hydroxamic acids, detoxification of chemical warfare stimulants, and reactivation kinetics of organophosphate-inhibited acetylcholinesterase by oxime reactivators.

Manmohan L. Satnami is an Assistant Professor with the School of Studies in Chemistry, Pt. Ravishankar Shukla University, Raipur, India. Recently, he has been awarded the U.G.C. Research Award, New Delhi, India. His research interests include physical organic chemistry, catalysis, surface chemistry, nanomaterials, and micellar catalysis.